INTERNATIONAL JOURNAL OF INTEGRATED ENGINEERING
ISSN: 2229-838X e-ISSN: 2600-7916

IJIE

Vol. 16 No. 6 (2024) 58-69
https://publisher.uthm.edu.my/ojs/index.php/ijie

Correlation Effect on Different Temperature-Humidity Range of Highly Thermal GNP/AG/ SA Conductive Ink

Norida Mohammad Noor[1,2], Mohd Azli Salim[2]*, Nor Azmmi Masipan[2], Adzni Md. Saad[2], Chonlatee Photong[3], Mohd Zaid Akop[2]

[1] *Department of Mechanical Engineering, Politeknik Ungku Omar, MALAYSIA*
[2] *Fakulti Teknologi dan Kejuruteraan Mekanikal, Universiti Teknikal Malaysia Melaka, MALAYSIA*
[3] *Faculty of Engineering, Mahasarakham University, THAILAND*

*Corresponding Author: azli@utem.edu.my
DOI: https://doi.org/10.30880/ijie.2024.16.06.006

Article Info

Received: 17 May 2024
Accepted: 30 June 2024
Available online: 9 October 2024

Keywords

Graphene nanoplatelet (GNP), silver flakes (Ag), silver acetate (SA), hybrid conductive ink, temperature, humidity, cyclic test

Abstract

The study evaluates how the resistivity and properties of the material change in response to environmental factors such as temperature and humidity, and how these changes impact its performance in various applications. In order to develop a highly thermal graphene hybridization conductive ink, a new formulation of conductive ink was formulated using graphene nanoplatelet (GNP), silver flake (Ag), and silver acetate (SA) as conductive fillers mixed with organic solvents. The batch of chemicals was converted into a powder by undergoing sonication and stirring to create a powdery state. The powder was then treated with organic solvents, specifically 1-butanol and terpineol, and mixed using a thinky mixer to form a paste. The GNP/Ag/SA hybrid conductive ink paste was then printed on copper substrates using a mesh stencil and was cured at 250°C for 1 hour. Cyclic testing had been conducted using a cyclic bending test machine and a cyclic torsion test machine in a heat chamber with different temperature-humidity. The new formulation then was characterized base on the electrical and mechanical behaviour. After the torsion and bending tests, the GNP/Ag/SA hybrid conductive ink formulation reliability was evaluated. GNP/Ag/SA hybrid conductive ink room temperature baseline and GNP/Ag/SA hybrid conductive ink after given different temperature-humidity were compared in terms of electrical and mechanical properties. Both cyclic bending and torsion testing results showed an increasing value of resistance and resistivity with every progress of bending and torsion cycle, which displays a clear trend. The results indicate that the average resistance values at all sample points either stay constant or decrease with the increasing temperature. This observation suggests that the ink's electrical conductivity remains rather stable as the temperature increases. Thus, even with rising temperatures, the ink's electrical conductivity remains stable, indicating the ink's capacity to preserve its integrity and structural qualities within a defined temperature range. Future research should focus on improving the adhesion, stability and reliability of stretchable conductive inks under various temperature and humidity conditions.

1. Introduction

In recent years, the development of flexible and stretchable electronics has garnered significant interest due to its potential applications in various fields, including electrical devices, biomedical devices, and flexible displays [1, 2]. One of the key components of these devices is stretchable conductive ink, which allows for the transmission of electrical signals even when the material is subjected to deformation [2]. The main characteristics of stretchable conductive ink are its flexibility and expandability, and its ability to retain low resistance levels [3]. Despite its potential application, establishing thermal conductivity in electrical devices and high-power semiconductors has become a crucial technological challenge [2, 4]. The traditional use of soldering in die-attach techniques carries a risk of thermal stress because of the substantial disparities in thermal expansion coefficients between the die and the substrate [5]. Furthermore, constraints on die height stem from the limited amount of solder that may be used for application, leading to a shift towards developing composite materials for electronic pastes, especially in applications that need high thermal conductivity.

The GNP, Ag, and SA are three materials that have shown great promise in the field of conductive inks due to their high conductivity, flexibility, and ease of processing. Graphene shows great potential due to its exceptional thermal conductivity, electrical conductivity, and mechanical strength [6]. Graphene also has been extensively studied because of its outstanding electrical and mechanical properties, making it a highly desirable material for creating conductive inks. However, pure graphene inks often exhibit low electrical conductivity, which limits their suitability for use in printed electronics applications [2]. The incorporation of metallic nanoparticles into graphene-based conductive inks has garnered attention as a strategy to enhance the intrinsic properties of graphene. Silver is selected as a filler for its more effective properties as a conductive ink and adhesion compared to other electrically conductive fillers. This is due to its high electrical and thermal conductivities, chemical stability, and the conductivity of its oxide form [7]. Additionally, silver has a low melting point, which is important for applications involving flexible substrates since it encourages the creation of conductive thin films at comparatively low temperatures [8-10].

Various research studies conducted experiments with varying temperatures, both higher and lower, on conductive ink. Most of the findings indicated that the resistance of the conductive ink decreases as the temperature rises when exposed to high temperatures [11-12]. According to [13], the printed film's conductivity improves with the increasing temperature and sintering time, and the SEM micrographs display more compact microstructures and larger coarsening grains [11, 13, 14]. The coarse grains allow electron transfer between grains, leading to a reduction in the resistivity of conductive ink. Silver ink performed better at higher curing temperatures, with the lowest sheet resistance recorded at 105°C. An opposite trend was seen with graphite ink, with resistivity decreasing during low temperature curing at 50°C. Ink with a larger concentration of silver exhibited improved conductivity at elevated temperatures, while ink with a higher quantity of graphite shown superior conductivity at lower temperatures [13, 15].

Advancements in mechanics and materials now enable the creation of integrated circuits with electrical capabilities akin to those of conventional rigid circuits, while also possessing the ability to stretch, compress, twist, bend, and mold into various forms [16]. The GNP-based conductive ink printed on substrates showed consistent high electrical conductivity even after undergoing severe bending cycles following thermal reduction [11]. In addition to electrical properties, mechanical characteristics of stretchable conductive inks are also important for their practical applications. Therefore, cyclic testing such as stretch, bending and torsion are commonly used to evaluate the mechanical properties of these materials. When printed conductive ink undergoes single or repetitive deformation such stretch, bending, and torsion, the flexible conductors deform significantly between the film and the substrate, leading to a reduction in device performance. High-quality conductive ink should maintain its functionality even after enduring numerous repetitive deformations caused by body movements [17].

This research focuses on the relationship between temperature and humidity on the electrical and mechanical properties of a highly thermal GNP/Ag/SA conductive ink. The findings of this study provide insights into the electrical and mechanical properties of ink under different environmental conditions, which is important for the development of more reliable and stable stretchable electronics.

2. Material and Methods

2.1 Material

The formulation of highly thermal GNP hybridization consists of GNP, Ag and SA as the filler, ethanol as the chemical solvent, and I-Butanol and terpineol as the organic solvents as shown in Table 1.

2.2 Substrate Preparation

Copper was used as the substrate because of its high density, high thermal conductivity, and high specific heat capacity. Copper is also recognised for its outstanding physical and chemical qualities, including heat conductivity

Int. Journal of Integrated Engineering Vol. 16 No. 6 (2024) p. 58-69

of 400 W/(m•K), electrical conductivity of 58 × 10^6 S/m, and corrosion resistance. [18, 19, 20]. Metal base substrates are frequently used in electronic devices that demand great performance, including high-frequency circuit boards, power electronics, and high-temperature applications.

The copper substrates were used as received and were cut according to the size needed. The dimensions of the substrate are 120 mm (*l*), 7 mm (*w*), and 0.1 mm (*t*). To prevent the copper substrates from oxidizing, it was etched with sandpaper. Six (6) pieces of cooper substrate were prepared for this research. Each substrate was then marked with 20mm between each mark for the printing process, as shown in Fig. 1.

Table 1 *Composition of different constituents' mixture according to the weight for 1 set*

	GNP (g)	Silver Flake (g)	Silver Acetate (g)	Ethanol (ml)	I-Butanol (drop)	I-Terpineol (drop)
1 set	0.05	0.4292	0.042	5	3	3

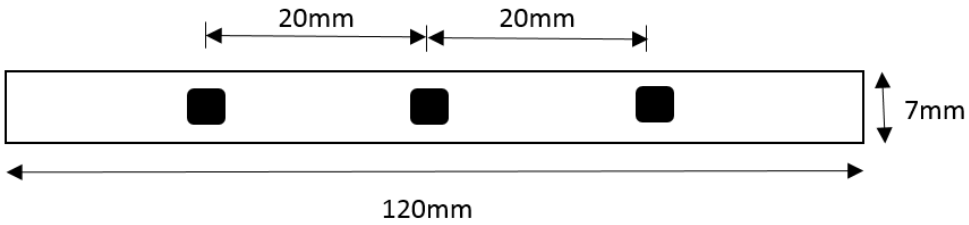

Fig. 1 *Dimension of the cooper substrate*

2.3 Formulation Development of GNP Hybrid

With the aim of developing a highly thermal graphene hybridization conductive ink, a new formulation of conductive ink was formulated using GNP, Ag, and SA as conductive fillers mixed with organic solvents. To turn the batch of substances into a powder, they were sonicated and followed by stirring to form the mixture into a powder. At room temperature mixture powder was pound until it produced a fine powder. Before curing at 250°C for 1 hour, the powder was dripped with organic solvents, 1-butanol, and terpineol and mixed using a thinky mixer machine to form a paste.

2.4 Printing Method Process

The GNP hybrid paste was printed on copper substrates using a mesh stencil as shown in Fig. 2. The mesh stencil has a thickness of 10 µm. The hybrid GNP paste was placed on the selected grid (3mm x 3mm) and applied using a squeegee. The paste was printed on the three selected points of the substrate strip. After the printing was completed, the mesh stencil was cleaned, and the process was repeated on each sample.

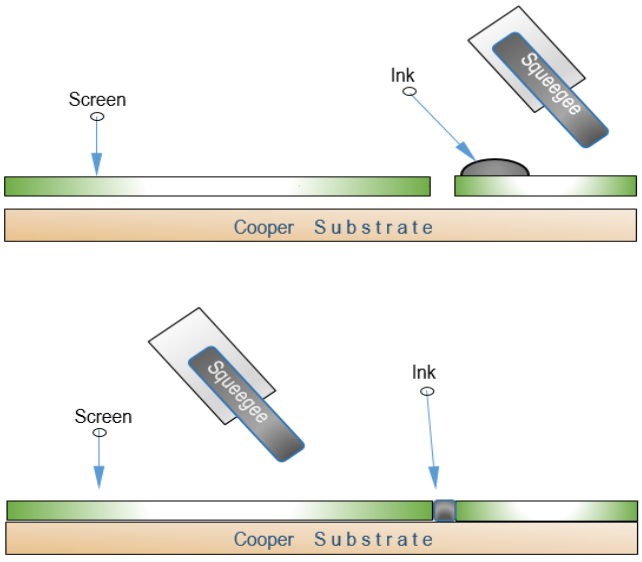

Fig. 2 *Printing process using the mesh stencil*

2.5 Cyclic Bending Test

Cyclic testing was performed through a cyclic bending test machine and a cyclic torsion test machine. The cyclic test was conducted following the guidelines of ASTM D7774-17, utilizing a three-point loading technique. Durability of conductive ink was assessed by cyclic bending and torsion tests conducted both before and after the experiment. The resistivity of the conductive ink is determined when the process is completed.

In this research the cyclic bending test machine was placed in a heat chamber. The testing was done based on different temperature-humidity. Each number of lamps resulted in different temperature and humidity. Once the reading from the temperature and humidity sensor stable in the heat chamber, the test was done starting with 1000 cycles, 3000 cycles and 5000 cycles, respectively. Once the counter hits 1000 cycles, resistance measurements were taken using a Two-Point probe. This procedure was repeated for 3000 cycles and 5000 cycles.

The samples were printed at three different points on the copper substrate. After the bending process, the resistivity and physical condition of the surface at these three points were compared. To bend the samples, the substrate was held firmly at both ends while only one end was free to bend. A 12 V DC motor on the bending test equipment rotated the wheel and connected the sample holder, bending the sample along the rail. As shown in Fig. 3, a cyclic bending test machine was used to measure the durability of the sample.

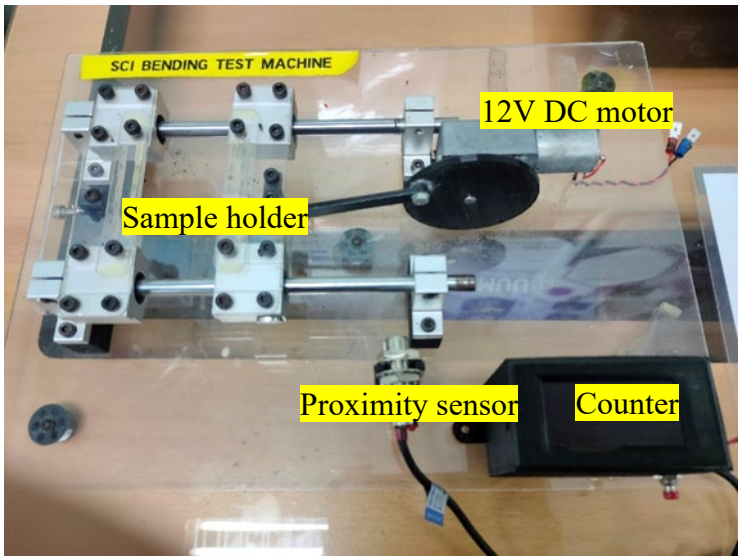

Fig. 3 *Cyclic bending test machine*

2.6 Cyclic Torsion Test

The sample preparation for the cyclic torsion test was similar to the bending test sample preparation except for the primary mode of deformation involves twisting, with conductive ink printed at three separate points on a copper substrate to determine the physical condition and resistivity value after twisting. The twisting motion of the samples was caused by two holders, with one remaining stationary while the other repeatedly rotated. During the tests, the twisting deformation was first rotated in a clockwise direction, then in the opposite direction, with a twisting angle of ± 90°. Fig. 4 shows the cyclic bending test machine.

2.7 Heat Chamber

The values of temperature and humidity in this research are based on the number of lamps switched on in the heat chamber as shown in Fig. 5. The heat chamber has six (6) lamps. Different temperature and humidity levels are gained by turning on two (2) lamps, four (4) lamps, and six (6) lamps, respectively, in the chamber. The temperature and humidity readings are obtained by using a temperature and humidity sensor, as shown in Table 2.

3. Results and Discussion

Cyclic testing had conducted using a cyclic bending test machine and a cyclic torsion test machine in a heat chamber with different temperature-humidity was used to analyze the resistivity of GNP/Ag/SA hybrid conductive ink. Cyclic testing involves subjecting a sample to repeated cycles of stress, to simulate real-world use and identify potential failure points. In terms of durability following cyclic bending and cyclic torsion tests, observations were made at all three points and a comparison was performed between before and after the cyclic

Int. Journal of Integrated Engineering Vol. 16 No. 6 (2024) p. 58-69

bending and cyclic torsion processes. GNP/Ag/SA hybrid conductive ink room temperature baseline and GNP/Ag/SA hybrid conductive ink hybrid after given different temperature-humidity were compared in terms of electrical and mechanical properties. The purpose of the cyclic bending and cyclic torsion tests is to ensure the reliability of the GNP/Ag/SA hybrid conductive ink. The device's reliability and lifetime are important because mechanical stresses caused by mechanical elastic deformation of the substrate can lead to rapid degradation of system performance [21].

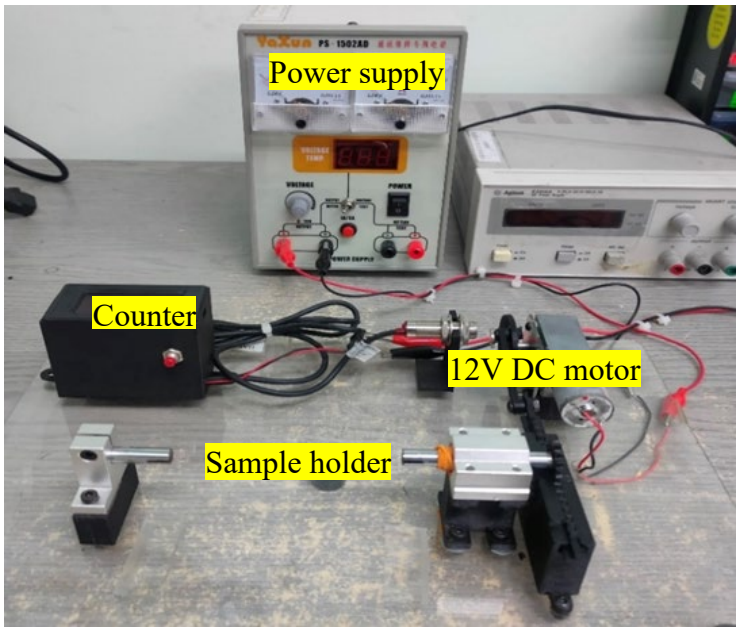

Fig. 4 *Cyclic torsion test machine*

Fig. 5 *Heat chamber*

Table 2 *Value of temperature and humidity*

Number of Lamps	Temperature ^{o}C	Relative Humidity %
0	21.6	80.5
2	25.2	72.4
4	28.6	64
6	30.6	60.8

3.1 Cyclic Torsion Test

Table 3 shows the resistance and resistivity measurement data for 1000, 3000, 5000 cycles of bending and torsion testing respectively. Resistivity value increases with the increment of numbers of cycle for both testing. The resistivity reading at cycle 1000 for bending test indicates the stability of the conductive ink. The highest resistivity value is at cyclic torsion test at 5000 cycles at point three (3) with 11.78 x 10-6 ohm.m with 21.86% of resistivity percentage change.

Table 3 *Resistance and resistivity of GNP hybrid at temperature 25.2°C - humidity 72.4%*

Cyclic Test	Sample	Cycle	Pattern Number	Average resistance at room temperature (Ω)	Average resistivity at room temperature (Ω.m)	Average resistance at different temperature - humidity (Ω)	Average resistivity resistance at different temperature-humidity (Ω.m)	Standard deviation (Ω.m)	Resistivity percentage change (%)
Cyclic Bending Test	Sample 1 (Temperature 25.2°C - Humidity 72.4%)	1000 cycle	Point 1	1.0556	10.56×10^{-6}	1.0556	10.56×10^{-6}	1.92×10^{-7}	0.00
			Point 2	1.1111	11.11×10^{-6}	1.0444	10.44×10^{-6}	3.85×10^{-7}	-6.00
			Point 3	1.0111	10.11×10^{-6}	1.0111	10.11×10^{-6}	1.92×10^{-7}	0.00
		3000 cycle	Point 1	1.0556	11.89×10^{-6}	1.056	10.56×10^{-6}	1.90×10^{-7}	0.04
			Point 2	1.1111	10.67×10^{-6}	1.022	10.22×10^{-6}	6.90×10^{-7}	-8.02
			Point 3	1.0111	9.67×10^{-6}	1.056	10.56×10^{-6}	1.90×10^{-7}	4.44
		5000 cycle	Point 1	1.0556	10.44×10^{-6}	1.044	10.44×10^{-6}	3.80×10^{-7}	-1.10
			Point 2	1.1111	10.22×10^{-6}	1.089	10.89×10^{-6}	3.80×10^{-7}	-1.99
			Point 3	1.0111	10.33×10^{-6}	1.089	10.89×10^{-6}	8.40×10^{-7}	7.70
Cyclic Torsion Test	Sample 2 (Temperature 25.2°C - Humidity 72.4%)	1000 cycle	Point 1	1.1889	11.11×10^{-6}	1.067	10.67×10^{-6}	3.30×10^{-7}	-10.25
			Point 2	1.0667	11.11×10^{-6}	1.056	10.56×10^{-6}	5.10×10^{-7}	-1.00
			Point 3	0.9667	10.22×10^{-6}	1.0556	10.56×10^{-6}	5.09×10^{-7}	9.20
		3000 cycle	Point 1	1.1889	10.44×10^{-6}	1.089	10.89×10^{-6}	3.80×10^{-7}	-8.40
			Point 2	1.0667	10.67×10^{-6}	1.067	10.67×10^{-6}	6.70×10^{-7}	0.03
			Point 3	0.9667	10.67×10^{-6}	1.089	10.89×10^{-6}	6.90×10^{-7}	12.65
		5000 cycle	Point 1	1.1889	10.56×10^{-6}	1.089	10.89×10^{-6}	3.80×10^{-7}	-8.40
			Point 2	1.0667	10.33×10^{-6}	1.111	11.11×10^{-6}	3.80×10^{-7}	4.15
			Point 3	0.9667	10.78×10^{-6}	1.178	11.78×10^{-6}	8.40×10^{-7}	21.86

Based on Fig. 6, it can be observed that the value of resistivity increases with the increment of the number of cycles for both tests. The values of resistance and resistivity for the cyclic torsion test are slightly higher than those for the bending test, in the cyclic torsion test, the material is subjected to alternating torsional loads. During a cyclic torsion test, the material experiences alternating torsional loads by the repetitive application of twisting or rotating force in opposite directions. This typically occurs with a specialised testing device designed for torsional testing, like a cyclic torsion testing machine. During the testing period, the GNP/Ag/SA hybrid conductive samples is secured at both ends and subjected to a torsional strain by rotating one end while keeping the other end stationary.

Int. Journal of Integrated Engineering Vol. 16 No. 6 (2024) p. 58-69

The twisting action creates shear stresses in the material, leading to deformation. Then, the rotation direction is reversed, applying an opposing torsional load to the material. The cyclic loading method is performed numerous times to mimic torsional fatigue effects on the material. This generates complex stress and strain patterns in the material that can result in higher levels of material damage compared to bending tests, leading to higher resistivity. The increase in resistivity is more significant in torsion tests due to the complex stress and strain patterns generated in the material [22]. During cyclic torsion deformation, the GNP/Ag/SA hybrid conductive ink samples experience a twisting motion that leads to a more even distribution of stresses and strains across the sample. Table 4 shows the resistance and resistivity measurement data for 1000, 3000, 5000 cycles of bending and torsion testing respectively at Temperature 28.6°C - Humidity 64%. At cyclic bending test, the average resistivity increases at all points along with the amount of bending cycle. At cyclic torsion test, increment of resistance and resistivity can be observing except for cycle 1000, point 1 and 2 and cycle 3000, point 2.

The variations in the electrical characteristics of the material across the substrate can be caused by the differences in the thickness of the ink layer. Uneven spacing may arise during the screen-printing process when the squeegee moves across the gap, potentially due to factors such as ink speed or viscosity. When the squeegee moves across the gap, there are some uneven spaces because of the speed or viscosity of the ink during the screen-printing process [23]. The squeegee transfers ink onto the substrate through a mesh screen, and changes in speed or ink thickness can impact the consistency of the ink layer. Differences in the thickness of the ink layer can cause variations in the electrical properties of the material, resulting in differences in conductivity or other electrical characteristics throughout the substrate. Controlling ink viscosity, printing speed, and screen alignment are essential for maintaining consistent electrical characteristics of the printed material.

Fig. 7 presents the resistance and resistivity values and their corresponding standard deviations for each sample at a temperature 31.6°C - humidity 60.8%. From the result shows that the same pattern where the resistance and resistivity of 5000 cycles is higher than 3000 and 1000 cycles. The prolonged cyclic loading over 5000 cycles compare to 3000 and 1000 cycles causes progressive material deterioration condition as stated in Euler and Bernoulli beam theories. Crack formation in the GNP/Ag/SA hybrid conductive sample was cause by the stresses on the surface. The stresses were caused by both bending moment and shear force. Cracks occurred in the samples when subjected to cyclic fatigue. As the cycle was increased, the crack extended and merged from both sides to create a fully extended crack across the ink width. Repeated bending and torsion stress on the sample led to stress concentration at the top surface [4].

During cyclic loading, the material experiences plastic deformation, which can lead to the formation of dislocations, grain boundary sliding, and other microstructural changes. Plastic deformation occurs when a material is subjected to cyclic loading, especially over its elastic limit. This indicates that when the load is released, the material does not revert to its initial form. The shape and structure of the material permanently alter as a result of plastic deformation. Plastic deformation in materials occurs because of the displacement of dislocations, which are linear imperfections in the crystal lattice of the material. Fig. 8 shows how edge dislocations accommodate shear stress by migrating through the crystal lattice. These changes can increase the scattering of electrons, leading to an increase in electrical resistance and resistivity [24].

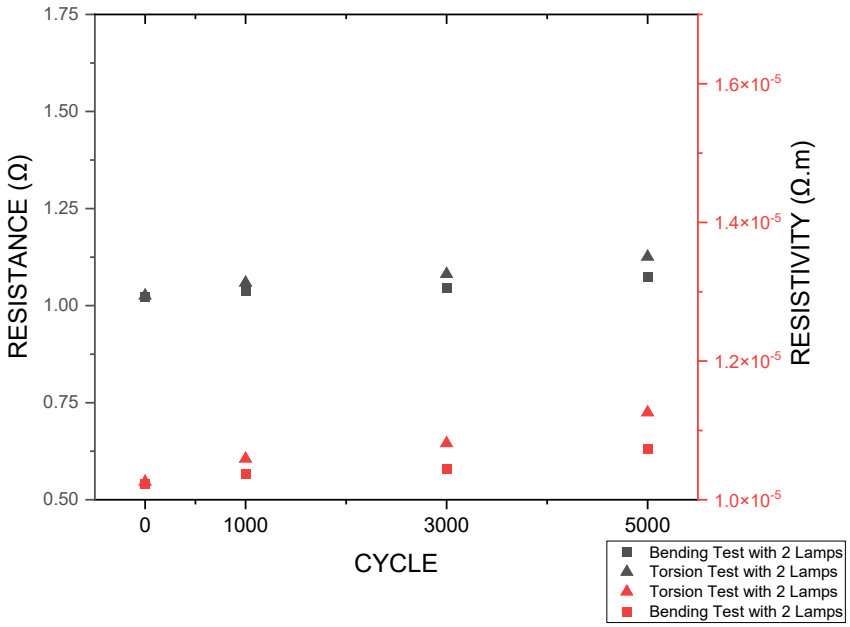

Fig. 6 *Resistance and resistivity of each cycle base on bending test and torsion test with temperature-humidity*

Table 4 *Resistance and resistivity of GNP hybrid at temperature 28.6°C - humidity 64%*

Cyclic Test	Sample	Cycle	Pattern Number	Average resistance at room temperature (Ω)	Average resistivity at room temperature (Ω.m)	Average resistance at different temperature - humidity (Ω)	Average resistivity resistance at different temperature-humidity (Ω.m)	Standard deviation (Ω.m)	Resistivity percentage change (%)
Cyclic Bending Test	Sample 1 (Temperature 25.2°C - Humidity 72.4%)	1000 cycle	Point 1	1.0444	10.44×10^{-6}	1.0778	10.78×10^{-6}	5.09×10^{-7}	3.20
			Point 2	1.0222	10.22×10^{-6}	1.0667	10.67×10^{-6}	6.67×10^{-7}	4.35
			Point 3	1.0333	10.33×10^{-6}	1.0556	10.56×10^{-6}	6.94×10^{-7}	2.16
		3000 cycle	Point 1	1.0444	10.44×10^{-6}	1.1	11.00×10^{-6}	5.80×10^{-7}	5.32
			Point 2	1.0222	10.22×10^{-6}	1.078	10.78×10^{-6}	8.40×10^{-7}	5.46
			Point 3	1.0333	10.33×10^{-6}	1.089	10.89×10^{-6}	1.90×10^{-7}	5.39
		5000 cycle	Point 1	1.0444	10.44×10^{-6}	1.133	11.33×10^{-6}	6.70×10^{-7}	8.48
			Point 2	1.0222	10.22×10^{-6}	1.1	11.00×10^{-6}	8.80×10^{-7}	7.61
			Point 3	1.0333	10.33×10^{-6}	1.111	11.11×10^{-6}	3.80×10^{-7}	7.52
Cyclic Torsion Test	Sample 2 (Temperature 25.2°C - Humidity 72.4%)	1000 cycle	Point 1	1.1111	11.11×10^{-6}	1.0889	10.89×10^{-6}	6.94×10^{-7}	-2.00
			Point 2	1.1111	11.11×10^{-6}	1.0889	10.89×10^{-6}	3.85×10^{-7}	-2.00
			Point 3	1.0222	10.22×10^{-6}	1.0778	10.78×10^{-6}	3.85×10^{-7}	5.44
		3000 cycle	Point 1	1.1111	11.11×10^{-6}	1.122	11.22×10^{-6}	1.90×10^{-7}	0.98
			Point 2	1.1111	11.11×10^{-6}	1.089	10.89×10^{-6}	3.80×10^{-7}	-1.99
			Point 3	1.0222	10.22×10^{-6}	1.111	11.11×10^{-6}	1.90×10^{-7}	8.69
		5000 cycle	Point 1	1.1111	11.11×10^{-6}	1.178	11.78×10^{-6}	1.90×10^{-7}	6.02
			Point 2	1.1111	11.11×10^{-6}	1.167	11.67×10^{-6}	0.00	5.03
			Point 3	1.0222	10.22×10^{-6}	1.178	11.78×10^{-6}	1.90×10^{-7}	15.24

Table 5 *Resistance and resistivity of GNP hybrid at temperature 30.6°C - humidity 60.8%*

Cyclic Test	Sample	Cycle	Pattern Number	Average resistance at room temperature (Ω)	Average resistivity at room temperature (Ω.m)	Average resistance at different temperature - humidity (Ω)	Average resistivity resistance at different temperature-humidity (Ω.m)	Standard deviation (Ω.m)	Resistivity percentage change (%)
Cyclic Bending Test	Sample 1 (Temperature 25.2°C - Humidity 72.4%)	1000 cycle	Point 1	1.0556	10.56×10^{-6}	1.4667	14.67×10^{-6}	3.33×10^{-7}	38.94
			Point 2	1.1111	11.11×10^{-6}	1.5222	15.22×10^{-6}	1.58×10^{-6}	37.00
			Point 3	1.0111	10.11×10^{-6}	1.4222	14.22×10^{-6}	1.92×10^{-7}	40.66
		3000 cycle	Point 1	1.1889	11.89×10^{-6}	1.478	14.78×10^{-6}	1.48×10^{-5}	24.32
			Point 2	1.0667	10.67×10^{-6}	1.544	15.44×10^{-6}	1.35×10^{-6}	44.75
			Point 3	0.9667	9.67×10^{-6}	1.444	14.44×10^{-6}	5.10×10^{-7}	49.37

	5000 cycle	Point 1	1.0444	10.44 x 10^{-6}	1.522	15.22 x 10^{-6}	1.90 x 10^{-7}	45.73
		Point 2	1.0222	10.22 x 10^{-6}	1.589	15.89 x 10^{-6}	9.60 x 10^{-7}	55.45
		Point 3	1.0333	10.33 x 10^{-6}	1.556	15.56 x 10^{-6}	5.10 x 10^{-7}	50.59
Cyclic Torsion Test Sample 2 (Temperature 25.2°C - Humidity 72.4%)	1000 cycle	Point 1	1.1111	11.11 x 10^{-6}	1.556	15.56 x 10^{-6}	1.90 x 10^{-7}	40.04
		Point 2	1.1111	11.11 x 10^{-6}	1.567	15.67 x 10^{-6}	0.00	41.03
		Point 3	1.0222	10.22 x 10^{-6}	1.556	15.56 x 10^{-6}	1.90 x 10^{-7}	52.22
	3000 cycle	Point 1	1.0444	10.44 x 10^{-6}	1.567	15.67 x 10^{-6}	3.30 x 10^{-7}	50.04
		Point 2	1.0667	10.67 x 10^{-6}	1.578	15.78 x 10^{-6}	1.90 x 10^{-7}	47.93
		Point 3	1.0667	10.67 x 10^{-6}	1.589	15.89 x 10^{-6}	6.90 x 10^{-7}	48.96
	5000 cycle	Point 1	1.0556	10.56 x 10^{-6}	1.656	16.56 x 10^{-6}	5.10 x 10^{-7}	56.88
		Point 2	1.0333	10.33 x 10^{-6}	1.678	16.78 x 10^{-6}	1.90 x 10^{-7}	62.39
		Point 3	1.0778	10.78 x 10^{-6}	1.667	16.67 x 10^{-6}	3.30 x 10^{-7}	54.67

The result in Table 5 shows the resistance and resistivity measurement data for 1000, 3000, 5000 cycles of bending and torsion testing respectively at Temperature 30.6°C - Humidity 60.8%. The resistivity percentage changes compared to resistivity at room temperature are in the range of 24% to 62% showing increment of resistivity at every point of each sample. As mentioned earlier, repeated stress from bending and torsion can cause dislocations within the material. The significant increase in dislocation density and dispersion caused by the high imposed stress can be attributed to the resistivity increase after processed [25]. It can be observed that the percentage change of point number 2 in cyclic torsion test at 5000 cycles are the highest with 62.39% because it is in the most critical area, which is the notch tip of torsion [26].

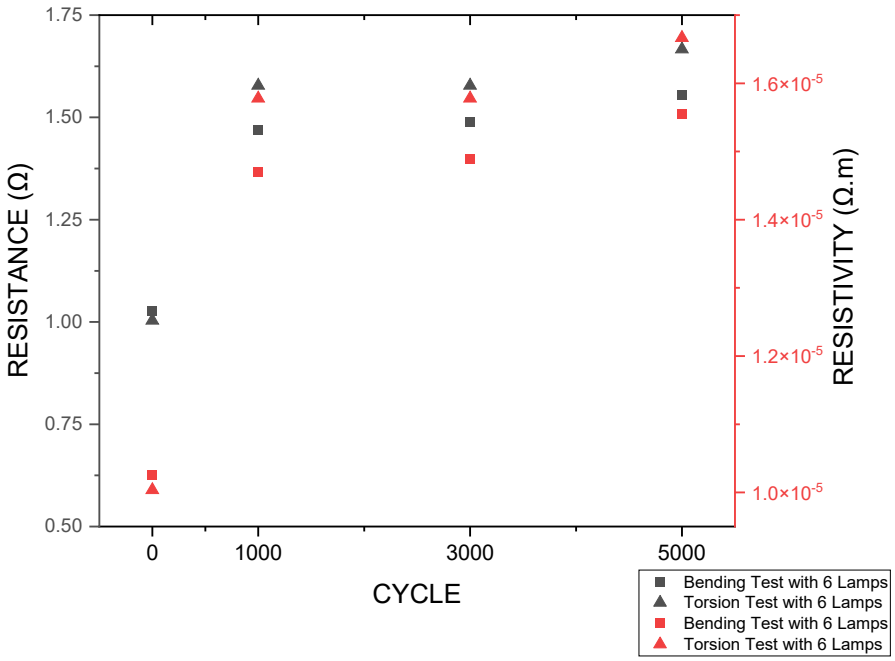

Fig. 9 *Measurement of resistance and resistivity of each cycle base on bending test and torsion test with temperature 30.6°C - humidity 60.8%*

Figure 9 illustrates the comparison measurement of resistance and resistivity for each cycle based on bending and torsion tests conducted at a temperature of 31.6°C and humidity of 60.8%. It can be observed that the value

of resistivity increases with the increasing number of cycles for both tests. This occurred because of the effect of the Euler-Bernoulli beam theory. The material was stretched during the bending and torsion cyclic tests, increasing the constriction and tunneling resistance because of the filler particles' increased distance, crack nucleation and propagation development [4]. A significant increment of resistivity can be observed at cycles 1000 for both tests. Elevated temperatures can have a significant impact on the electrical resistivity of the hybrid material. High temperatures can result in the degradation or oxidation of the graphene, which can negatively impact its electrical conductivity and increase the resistivity. A decrease in electrical conductivity and an increase in resistivity were observed with the increasing temperature due to the degradation or oxidation of the graphene [27]. Graphene is a carbon, which is composed of a layer of independent sp^2 hybrid carbon atoms and each carbon atom in graphene is bonded to three adjacent carbon atoms [28]. Graphene is susceptible to thermal breakdown at high temperatures, which potentially weakens the structural integrity of the graphene lattice. The breakdown of carbon-carbon bonds within the graphene structure is a primary cause of this degradation and oxidation, which can result in the creation of defects, including vacancies, edges, and structural disorder.

Cyclic testing involving variations in temperature and humidity can yield insights into the temperature-humidity dependent electrical resistivity of a material. By subjecting the material to a range of temperature-humidity conditions, it is possible to observe changes in its electrical resistivity as a function of temperature-humidity. This data holds significance in characterizing the material's temperature stability and offers valuable insights into its applicability for specific purposes.

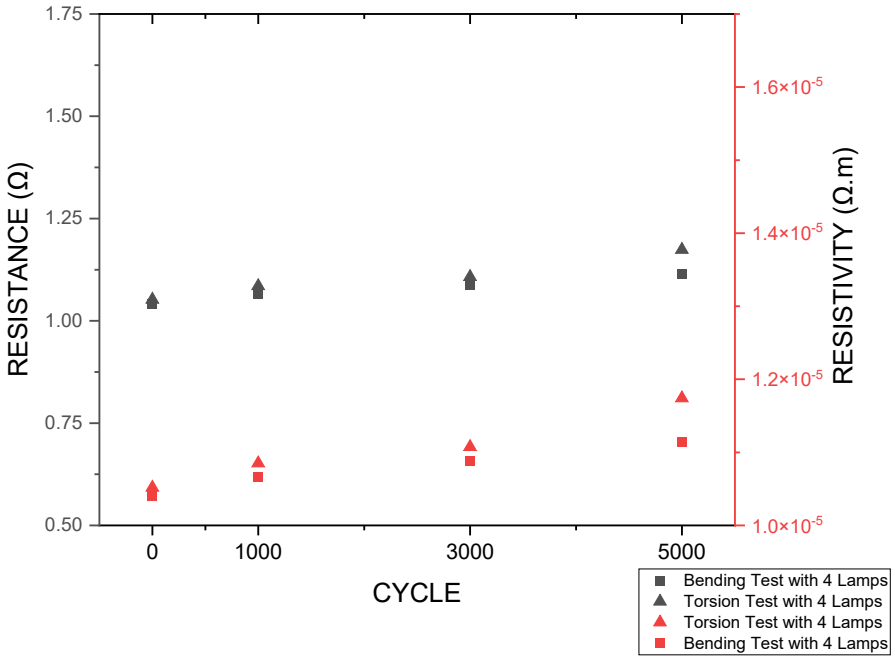

Fig. 7 *Resistance and resistivity of each cycle base on bending test and torsion test with temperature-humidity*

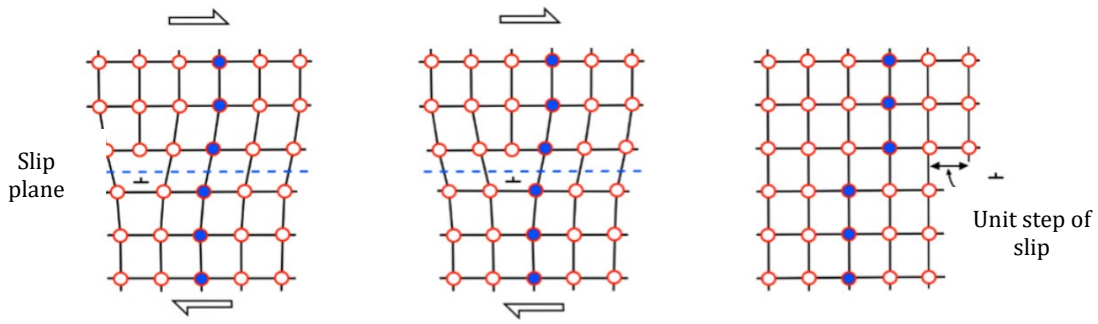

Fig. 8 *Migration of edge dislocation when shear stress is applied [29]*

4. Conclusion

The results of the correlational analysis show that electrical conductivity of the GNP/Ag/SA hybrid conductive is stable and consistent under standard and controlled conditions. Furthermore, the GNP/Ag/SA hybrid conductive demonstrates thermal stability, where resistivity value remains stable or decreases with the increasing temperature before the cyclic testing. This observation suggests that the ink's electrical conductivity remains rather stable as the temperature increases. It indicates ink's capacity to preserve its integrity and structural qualities within a defined temperature range.

The resistance and resistivity values demonstrate an incremental rise with each successive bending and torsion cycle under varying temperature-humidity conditions. Nevertheless, the conductive ink exhibits overall robustness, albeit with minor deleterious effects observed. The differences in temperature-humidity effects among the three distinct temperature-humidity conditions remained relatively consistent. However, a notable increase in resistance and resistivity was observed under the highest temperature condition (6 lamps). This significant rise in resistivity can be attributed to the heightened dislocation density and dispersion induced by the substantial stress imposed during processing. In conclusion, the stable electrical conductivity and thermal stability of the GNP hybrid conductive ink under standard and controlled conditions, along with its overall robustness despite minor deleterious effects observed during cyclic testing, affirm its suitability for various applications.

Acknowledgement

The authors would like to thank the Advanced Academia-Industry Collaboration Laboratory (AiCL) and Fakulti Teknologi dan Kejuruteraan Mekanikal, Engineering, Universiti Teknikal Malaysia Melaka (UTeM) for providing the laboratory facilities and its support.

Conflict of Interest

Authors declare that there is no conflict of interests regarding the publication of the paper.

Author Contribution

The authors confirm contribution to the paper as follows: ***study conception and design****: Norida Mohammad Noor, Mohd Azli Salim;* ***data collection****: Nor Azmmi Masripan;* ***analysis and interpretation of results****: Norida Mohammad Noor, Adzni Md. Saad;* ***draft manuscript preparation****: Norida Mohammad Noor, Mohd Azli Salim, Chonlatee Photong. Mohd Zaid Akop. All authors reviewed the results and approved the final version of the manuscript.*

References

[1] Wang Z, Sun L, Ni Y, Liu L and Xu W (2021). Flexible Electronics and Healthcare Applications. *Front. Nanotechnol. 3:625989.* https://doi: 10.3389/fnano.2021.625989

[2] Y.Z.N. Htwe, M. Mariatti (2022). Printed graphene and hybrid conductive inks for flexible, stretchable, and wearable electronics: Progress, opportunities, and challenges. *Journal of Science: Advanced Materials and Devices 7 (2022) 100435* https://doi.org/10.1016/j.jsamd.2022.100435

[3] Ameeruz Kamal Ab Wahid, Mohd Azli Salim, Nor Azmmi Masripan, Chonlatee Photong and Adzni Md. Saad (2021) Comparison Measurements of Low Resistance and High Strength on Synthesis Graphene Conductive Ink Filled Epoxy. *International Journal of Nanoelectronics and Materials Volume 14 [333-342]*

[4] Norhisham Ismail, Mohd Azli Salim, Azmi Naroh, Adzni Md. Saad, Nor Azmmi Masripan, Crtomir Donik, Ghazali Omar and Feng Dai (2020) The Behaviour of Graphene Nanoplatelates Thin Film for High Cyclic Fatigue. *International Journal of Nanoelectronics and Materials*

[5] Luchun Yan, Jiawen Yao, Yu Dai, Shanshan Zhang, Wangmin Bai, Kewei Gao, Huisheng Yang and Yanbin Wang (2022) Study of Thermal Stress Fluctuations at the Die-Attach Solder Interface Using the Finite Element Method. *Electronics 2022, 11, 62.* https://doi.org/10.3390/electronics11010062

[6] Deng, S., Zhang, X., Xiao, G.D., Zhang, K., He, X., Xin, S., Liu, X., Zhong, A. and Chai, Y., (2021). Thermal interface material with graphene enhanced sintered copper for high temperature power electronics. *Nanotechnology, 32(31), p.315710.*

[7] Iara J. Fernandes, Angélica F.Aroche, Ariadna Schuck, Paola Lamberty, Celso R. Peter, Willyan Hasenkamp and Tatiana L.A. C. Rocha (2020). Silver nanoparticle conductive inks: synthesis, characterization, and fabrication of inkjet-printed fexible electrodes. *Scientific Reports 10:8878* https://doi.org/10.1038/s41598-020-65698-3

[8] Kate Black, Jetinder Singh, Danielle Mehta, Sarah Sung, Christopher. J. Sutcliffe & Paul. R. Chalker (2016). Silver Ink Formulations for Sinter-free Printing of Conductive Films. *Scientific Reports | 6:20814*

DOI: 10.1038/srep20814
[9] Rao, V. K., Venkata, A., Karthik, P. S. & Singh, S. P. (2015). Conductive silver inks and their applications in printed and fexible electronics. *RSC Adv. 5, 77760–77790*
[10] Liu, J., Yu, S., Yin, Y. & Chao, J. (2012). Methods for separation, identifcation, characterization and quantifcation of silver nanoparticles. *TrAC Trends Anal. Chem. 33, 95–106*
[11] Salam, B. et al. (2011) 'Low temperature processing of copper conductive ink for printed electronics applications', *2011 IEEE 13th Electronics Packaging Technology Conference, EPTC 2011, (1), pp. 251–255.*
[12] G. Wang, Z. Wang, Z. Liu, J. Xue, G. Xin, Q. Yu, J. Lian, M.Y. Chen, (2015) Annealed Graphene Sheets Decorated with Silver Nanoparticles for Inkjet Printing, *Chem. Eng. J. 260*
[13] Mou, Y. et al. (2018) Fabrication of Highly Conductive and Flexible Printed Electronics by Low Temperature Sintering Reactive Silver Ink, *Applied Surface Science. Elsevier, 459(July), pp. 249–256.*
[14] Huang, L. et al. (2011) Graphene-Based Conducting Inks for Direct Inkjet Printing of Flexible Conductive Patterns and Their Applications in Electric Circuits and Chemical Sensors. *Nano Research, 4(7), pp. 675–684.*
[15] Joshi, S. S. (2011) 'Evaluation of Silver / Graphite Ink Blends for Use in Printed Electronics'.
[16] Ab Wahid, A.K., Salim, M.A., Masripan, N.A., Saad, A.M., Dobrota, D., Omar, G., Sudin, M.N. and Naroh, A., (2020) Driving Monitoring System Application with Stretchable Conductive Inks: A Review. *International Journal of Nanoelectronics & Materials, 13, 327-346.*
[17] Park, J. Y., Lee, W. J., Kwon, B.-S., Nam, S.-Y., and Choa, S.-H. (2018). Highly Stretchable and Conductive Conductors Based On Ag Flakes and Polyester Composites*. Microelectronic Engineering, 199, pp.16-23.*
[18] Jadhav, S.D., Dadbakhsh, S., Vleugels, J., Hofkens, J., Van Puyvelde, P., Yang, S., Kruth, J.P., Van Humbeeck, J., and Vanmeensel, K. (2019) Influence of Carbon Nanoparticle Addition (And Impurities) On Selective Laser Melting of Pure Copper. *Materials 2019, 12, 2469.*
[19] Ikeshoji, T.T., Nakamura, K., Yonehara, M., Imai, K., and Kyogoku, H. (2018) Selective Laser Melting of Pure Copper. *JOM 2018, 70, 396–400.*
[20] Mao, Z., Zhang, D.Z., Wei, P., and Zhang, K. (2017) Manufacturing feasibility and forming properties of Cu-4Sn in selective laser melting. Materials 2017, 10, 333.
[21] Jeong, H. Y., Lee, Y. H., Kim, T. W., & Cho, K. J. (2017). Design and Reliability of Flexible Devices. *Nano Convergence, 4(1), 23.*
[22] Zhang, J., Cheng, L., Li, X., Yang, Y., & Sun, R. (2018). Mechanical and Electrical Properties of Flexible Hybrid Films Based On Silver Nanowires and Graphene Oxide. *Nanomaterials, 8(10), 795*
[23] Zavanelli, N., & Yeo, W. H. (2021) Advances in Screen Printing of Conductive Nanomaterials for Stretchable Electronics. *In ACS Omega (Vol. 6, Issue 14, pp. 9344–9351). American Chemical Society.*
[24] Sundaram, A. K., Singh, H., & Lee, J. H. (2021). The Influence of Cyclic Loading On Electrical Conductivity and Resistivity of Materials: A Review. *Journal of Materials Science, 56(8), 4549-4577.*
[25] Kocich, R., Kunčická, L., Král, P. and Macháčková, A., (2016) Sub-Structure and Mechanical Properties of Twist Channel Angular Pressed Aluminium. *Materials Characterisation, 119, pp.75-83*.
[26] Suksangpanya, N., Yaraghi, N.A., Pipes, R.B., Kisailus, D. and Zavattieri, P., (2018) Crack Twisting and Toughening Strategies in Bouligand Architectures. *International Journal of Solids and Structures, 150, pp.83-106.*
[27] Liu, J., Liu, H., Liu, Y., Zou, J., Zhao, Y., & Zhang, K. (2021). Influence of Temperature On Electrical Conductivity and Electromagnetic Interference Shielding Effectiveness of Graphene-Based Composites. *Journal of Materials Science: Materials in Electronics, 32(13), 18636-18648.*
[28] Wang Yu, Li Sisicd, Yang Haiyana and Luo Jiee (2020) Progress in The Functional Modification of Graphene/Graphene Oxide: A Review. *RSC Adv., 2020, 10, 15328–15345.* DOI: 10.1039/d0ra01068e
[29] Passchier, C.W. and Trouw, R.A.J. (2005) Microtectonics. *2nd Edition, Springer, Berlin, 366 p*.